GEOPHYSICAL RESEARCH LETTERS, VOL. 39, L02304, doi:10.1029/2011GL050177, 2012

Magnetotelluric imaging of upper-crustal convection plumes beneath the Taupo Volcanic Zone, New Zealand

E. A. Bertrand,[1] T. G. Caldwell,[1] G. J. Hill,[1] E. L. Wallin,[1,2] S. L. Bennie,[1] N. Cozens,[1,3] S. A. Onacha,[4] G. A. Ryan,[4] C. Walter,[4] A. Zaino,[4] and P. Wameyo[4]

Received 4 November 2011; revised 19 December 2011; accepted 22 December 2011; published 21 January 2012.

[1] Broadband MT (magnetotelluric) data were recorded that form an array of measurements at the south-eastern margin of the TVZ (Taupo Volcanic Zone), in the central North Island of New Zealand. These array data are used to investigate mechanisms by which the TVZ's extraordinarily high heat flux is transported to the surface. Taken together with seismological data, these MT data show compelling evidence that support a model of hydrothermal convection within the brittle (upper ∼6–7 km) part of the crust. Both 2-D and 3-D inversion models of these MT data show vertical low-resistivity zones that connect surface geothermal fields to an inferred magmatic heat source that lies below the brittle-ductile transition. **Citation:** Bertrand, E. A., et al. (2012), Magnetotelluric imaging of upper-crustal convection plumes beneath the Taupo Volcanic Zone, New Zealand, *Geophys. Res. Lett.*, *39*, L02304, doi:10.1029/2011GL050177.

1. Introduction

[2] The rhyolitic part of the Taupo Volcanic Zone (TVZ) in the central North Island of New Zealand discharges ∼4.2 GW of heat [*Bibby et al.*, 1995]. At upper crustal depths, *Bibby et al.* [1995] suggest that this heat flux is transported to the surface via convection in 23 high-temperature geothermal systems, each of which are marked by near-surface low-resistivity anomalies (Figure 1). The shallow (<3 km) geothermal fields are thought to represent the upper portion of rising, high-temperature convective plumes that extend down to depths of ∼8 km [*Bibby et al.*, 1995; *Kissling and Weir*, 2005; *McLellan et al.*, 2010]. However, much remains uncertain about the basement structure and mechanisms of heat transport at depths >3 km (the present maximum drilled depth).

[3] The geothermal fields in the TVZ provide ∼10% of New Zealand's electricity demand [*Bignall*, 2010], but development is currently limited to depths of 2–3 km. To maintain, or to increase this level of geothermal energy in the long term, production from depths >3 km will be required where temperatures may approach 400°C. The highest temperature yet encountered is 332°C at ∼3 km depth in the Rotokawa geothermal field [*Hunt and Harms*, 1990]. Seismicity recorded in the TVZ suggests that the brittle-ductile transition occurs at a depth of ∼6–7 km [*Bibby et al.*, 1995; *Bryan et al.*, 1999]. Therefore, basement rocks (greywacke and meta-sediments) between 3 and 7 km should be able to support fracture permeability and allow convective heat transport. However, no geophysical methods have yet imaged the proposed plumes that connect the surface geothermal systems to their underlying magmatic heat source.

[4] To investigate links between the deep magmatic heat source and the shallow hydrothermal systems, a research project that includes structural geology, experimental geochemistry, passive-seismic and magnetotelluric (MT) measurements was initiated in 2008 [*Bignall*, 2010]. The goal of the MT and passive-seismic surveys is to identify structures present within the basement rocks at depths between 3 and 7 km that advance our understanding of the processes that transport heat to the surface. This paper describes the MT data analysis and shows detailed 2-D and 3-D inverse resistivity models that image narrow, vertical zones of low-resistivity that may represent the convective plumes described by *Bibby et al.* [1995].

2. Data Collection and Analysis

[5] Previously, regional MT surveys of the central TVZ have imaged the crustal resistivity structure to depths of 30–40 km [*Ogawa et al.*, 1999; *Ingham*, 2005; *Heise et al.*, 2007, 2010]. In addition, closely-spaced MT and seismic surveys have been conducted locally at individual geothermal fields to investigate shallow structures (upper 3 km) motivated by commercial development [*Heise et al.*, 2008]. Here, we focus on detailed basement structure in the upper 10 km using a dense array of MT measurements.

[6] Using Phoenix MTU instruments, broadband (0.01–1000 s) MT data were recorded for 2 nights duration at 204 locations in the south-eastern TVZ during the spring months of 2009 and 2010. Measurements were made at ∼2 km intervals on a series of profiles forming a NW-SE rectangular array (25 × 35 km) that extends from the central rift axis to the south-eastern rift margin (Figure 1). These profiles are oriented perpendicular to the dominant geological and geoelectric strike directions of the TVZ (i.e. N45°E [*Heise et al.*, 2007]). Robust processing of the measured time-series data using a remote reference to reduce cultural EM noise [*Gamble et al.*, 1979] resulted in high-quality MT soundings at most sites occupied. Details regarding the complementary passive-seismic survey are included in the auxiliary material (Figure S1).[1]

[7] Prior to inversion modeling, the dimensionality of MT data must be assessed. The magnetotelluric phase tensor

[1]GNS Science, Lower Hutt, New Zealand.
[2]Now at Pacific Northwest National Laboratory, Richland, Washington, USA.
[3]Now at New Zealand Petroleum and Minerals, Wellington, New Zealand.
[4]IESE, University of Auckland, Auckland, New Zealand.

0094-8276/12/2011GL050177

[1]Auxiliary materials are available in the HTML. doi:10.1029/2011GL050177.

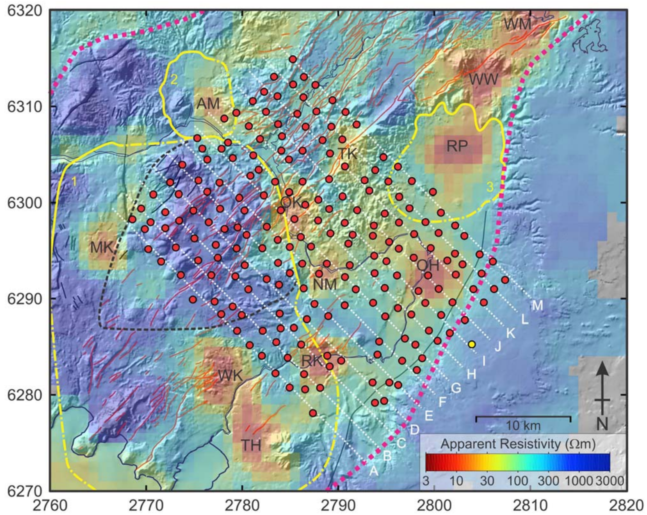

Figure 1. Map of the MT array in the south–eastern TVZ using the NZMG (New Zealand Map Grid) coordinate system (labels in km). Red circles are MT sites and the yellow circle the remote reference location. Profiles used in 2-D modeling are shown as white dashed lines (A to M). The background digital elevation model is overlain by the DC apparent resistivity map [*Bibby et al.*, 1995] that correlates low resistivity zones to geothermal systems: TH – Tauhara, WK – Wairakei, RK – Rotokawa, MK – Mokai, NM – Ngatamariki, OK – Orakei Korako, OH – Ohaaki, TK – Te Kopia, AM – Atiamuri, RP – Reporoa, WW – Waiotapu Waikiti, and WM – Waimungu. Yellow lines show collapsed caldera boundaries (1. Whakamaru, 2. Ohakuri, 3. Reporoa) that intersect the MT array; solid lines are constrained topographic margins while dashed lines are inferred structural collapse faults [*Wilson and Leonard*, 2008]. Black dashed line outlines the Maroa volcanic centre, and the pink dashed lines the eastern boundary of the TVZ after *Wilson et al.* [1995]. Active faults are shown as orange lines, other faults as black lines, and the Waikato River is outlined in blue.

[*Caldwell et al.*, 2004] provides an effective tool to investigate dimensionality that does not make any *a priori* assumptions regarding the regional resistivity structure. In addition, the phase tensor is not significantly affected by galvanic (static-shift) effects [*Caldwell et al.*, 2004] that bias the apparent resistivity data. Plotting the orientation of the maximum phase tensor principal axes ($\alpha - \beta$ values) for all periods measured at all sites in the present survey confirms that the overall geoelectric strike direction for these MT data is collinear to the major structural features in the TVZ (i.e. ~N45°E; Figure S2).

[8] Phase tensor ellipses can also be used as an indicator of MT data quality, since spatially coherent patterns should be observable between groups of neighboring sites. Phase tensor ellipses are plotted in Figure 2 (and at more periods in Figure S3) and show consistent patterns throughout the entire survey area and period range measured. For example, at 3s period (Figure 2) the phase tensors rotate 90° across the south-eastern boundary of the TVZ [*Wilson et al.*, 1995] and along the scarp of the Paeroa Fault. These rotations indicate along-strike boundaries between zones of low and high resistivity. Evidence of 3-D resistivity structure is also apparent as illustrated by the arcuate pattern in ellipses that follow the eastern boundary of the Whakamaru collapse caldera and the Maroa volcanic centre (Figure 2).

[9] In addition to the phase tensor, induction vectors (that are calculated from ratios of the vertical to horizontal magnetic field components) provide independent information on MT data dimensionality [*Parkinson*, 1962]. These vectors show overall 2-D behavior at short periods, but rotate to point north-east at periods greater than 100s (Figure S4). However, examination of the induction vectors shows that electromagnetic noise from high-voltage power transmission lines within the MT array clearly affect these data at periods less than ~10s (see auxiliary material for more detail). A similar examination of the phase tensor data does not show any correlation with the power-lines (Figure S3), indicating that this noise signal is restricted to the vertical magnetic fields, or that the remote reference processing has removed any effects from the impedance data. Inversion modeling presented below does not include the induction vector data.

3. Modeling and Interpretation

[10] Smooth 2-D resistivity models of the impedance data were generated for each profile in the array using the inversion algorithm of *Rodi and Mackie* [2001]. Obvious outliers and data points with large uncertainties were omitted manually prior to inversion. The models achieved acceptable normalized root mean square (r.m.s.) misfits between 1.2 and 1.5. Error floors were set to 10% for the apparent resistivity, and 5% for the phase. Setting a larger error floor for the apparent resistivity minimizes the effects of static shifts that do not affect the phase data [*Li et al.*, 2003]. Final 2-D resistivity models of each profile are included in Figure 3.

[11] All of the 2-D models in Figure 3 show a horizontal band of low-resistivity (10–30 Ωm) at depths ranging from the surface down to ~3 km. In places, this low-resistivity layer is overlain by more resistive material >300 Ωm. This shallow resistivity structure is similar to that inferred in previous MT surveys [*Ogawa et al.*, 1999; *Heise et al.*, 2007] and is interpreted as young (<~0.75 Ma) resistive volcanics

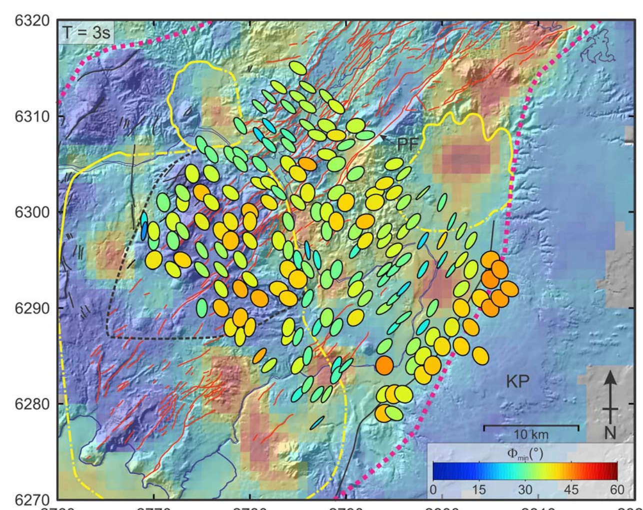

Figure 2. Measured phase tensor ellipses at a period of 3s, filled with color that shows the minimum phase (Φ_{min}) invariant. PF – Paeroa Fault, KP – Kaingaroa Plateau. All other labels as defined in Figure 1.

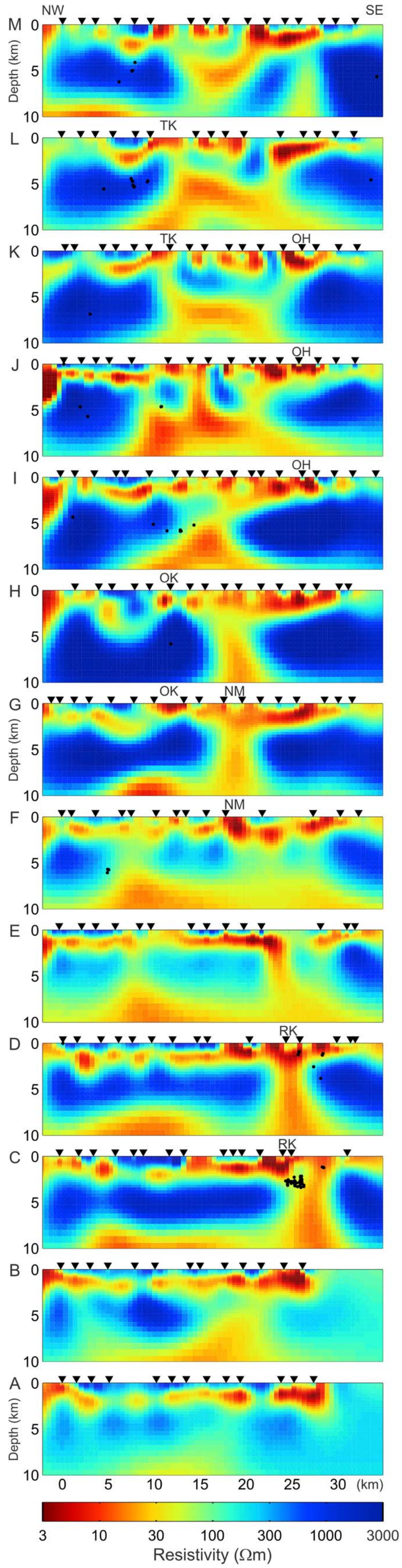

overlying older (>∼0.75 Ma) conductive materials. Conductive clays and zeolites are generated by diagenetic alteration and slowly interconnect throughout the rock matrix to lower the resistivity of old ignimbrites [*Stanley et al.*, 1990; *Bibby et al.*, 2005]. In general, high resistivity (∼1000 Ωm) is present from depths of ∼3 km down to ∼7–8 km, where the resistivity decreases to 10–30 Ωm.

[12] *Bibby et al.* [1995] propose that below the brittle-ductile transition, estimated from the cut-off in shallow seismicity at ∼6–7 km depth [also see *Bryan et al.*, 1999], heat transport occurs dominantly via conduction, supplemented by advection from sporadic magmatic intrusions. Regional MT models of the TVZ show low-resistivity at ∼10 km depth [*Heise et al.*, 2007], interpreted to represent a broad zone of ∼4% partial melt. This interpretation is consistent with inferred temperatures for TVZ magmas (730°C [*Nairn et al.*, 2004] and 820–850°C [*Sutton et al.*, 2000]). In profiles B to G in Figure 3 a broad area of low-resistivity (10–30 Ωm) occurs at depths greater than ∼7–8 km, shallower than previously suggested. This area is located beneath the Maroa volcanic center, where *Heise et al.* [2010] inferred a region of ponded melt to exist and which was active as recently as ∼60–30 ka [*Wilson et al.*, 1995].

[13] Superimposed on the background resistivity structure above ∼7–8 km depth, the 2-D models for several profiles show zones of low resistivity (∼10–30 Ωm) that connect surface geothermal fields to deeper low resistivity regions. In particular, at Rotokawa (RK) and Ngatamariki (NM), vertical low-resistivity zones extend from the near surface to broad low-resistivity regions at ∼7–8 km depth (profiles C, D, G in Figure 3). In contrast, at Ohaaki (OH) and Orakei Korako (OK), high resistivity occurs beneath the geothermal fields at depths beyond ∼3 km, and the connections between the near-surface low resistivity zones and the deeper low-resistivity regions are offset (profiles H, I, J in Figure 3). Although data coverage is sparse near Te Kopia (TK), the shallow low-resistivity zone that marks the geothermal field also appears to be connected to a broad region of low-resistivity at ∼5 km depth south-east of the Pearoa Fault (PF in Figure 2).

[14] Clearly, the along-strike variations between the resistivity models in Figure 3 are inconsistent with a 2-D modeling approach, although there is a good degree of profile-to-profile similarity. To validate the main resistivity structures seen in the 2-D models (especially the vertical low-resistivity zones) the 3-D MT inversion algorithm WSINV3DMT [*Siripunvaraporn et al.*, 2005] was used to model the MT data collected on profiles B, C, and D through the Rotokawa geothermal system, and separately for the MT data measured on profiles I, J and K through the Ohaaki geothermal system. See auxiliary material for details regarding the 3-D inversion modeling. Both the Rotokawa and Ohaaki models (Figure 4) converged after 8 and 5 iterations, respectively, with normalized r.m.s. misfits of 1.1. Note that this

Figure 3. 2-D resistivity inversion models of the profile MT data in Figure 1 that show low-resistivity plumes connected to several geothermal fields: RK – Rotokawa, NM – Ngatamariki, OK – Orakei Korako, OH – Ohaaki and TK – Te Kopia. Black dots show the projection of hypocenters of earthquakes occurring within 1 km on either side of the profiles.

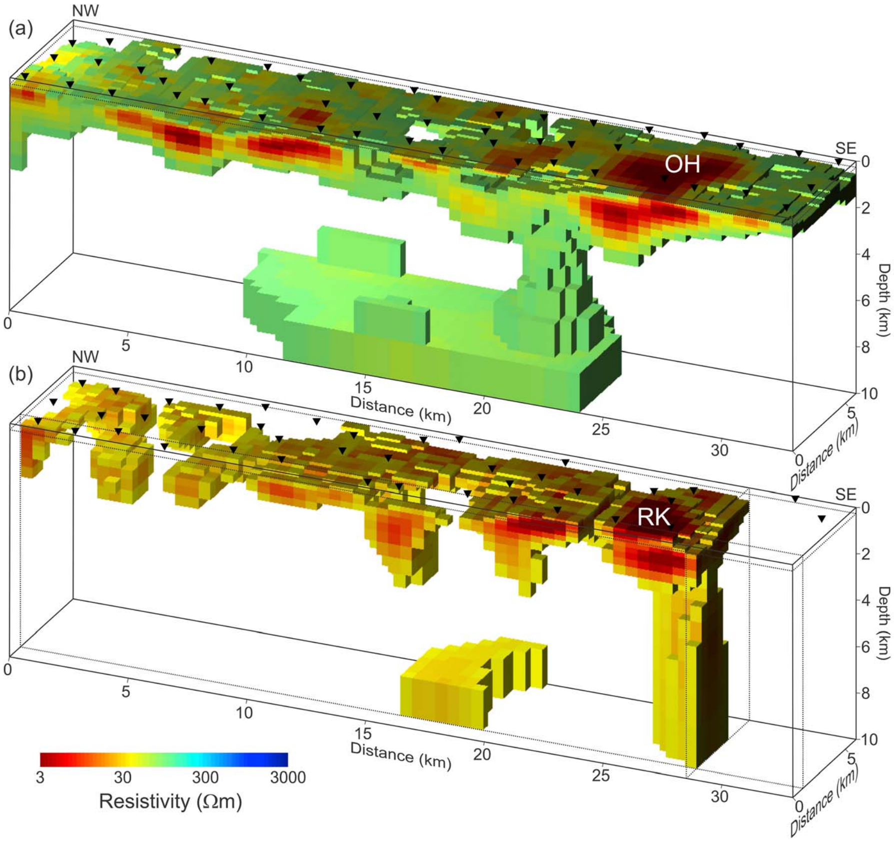

Figure 4. 3-D models of the full MT impedance tensor data for (a) profiles I, J and K through Ohaaki (OH) and (b) profiles B, C and D through Rotokawa (RK), as shown in Figure 1. A resistivity cut-off is used to permit a 3-D view of the vertical (RK) and offset to the north–west (OH) low-resistivity plumes that connect to the surface geothermal fields.

inversion algorithm does not solve for static shifts or include the effects of topography. However, the model resistivities at 250 m depth agree well with the DC apparent resistivity values [*Bibby et al.*, 1995], suggesting that static and topographic effects do not significantly influence these MT data (Figure S5).

[15] The 3-D models shown in Figure 4 confirm the existence of the low-resistivity zones that connect the near-surface hydrothermal systems at Rotokawa (vertical) and Ohaaki (offset to the north-west) to a low-resistivity layer at ∼7–8 km depth. In addition, a 3-D synthetic test (Figure S6) shows that a large effect on the phase tensor response occurs if these vertical conductors are removed. These resistivity models image for the first-time connections between the shallow (upper 3 km) parts of the known hydrothermal systems and their deeper underlying heat source.

4. Discussion

[16] What causes the vertical, low-resistivity structures in the MT models? The convective model of heat transport for the TVZ [*Bibby et al.*, 1995] envisages rising, narrow plumes of hot water (at near-hydrostatic pressures) beneath each of the geothermal fields. These plumes capture and concentrate the heat-flux from an inferred magmatic zone [∼1–4% partial melt; *Robinson et al.*, 1981; *Harrison and White*, 2006] at ∼10 km depth [*Heise et al.*, 2007, 2010]. The large areas between the plumes are inferred to be down-flow regions of cold meteoric water that are required to maintain convection. These areas have not been exposed to geothermal fluids and have never undergone hydrothermal alteration, suggesting that once formed, hydrothermal plumes are stable and long-lived [*Bibby et al.*, 1995].

[17] In general, the resistivity models in Figure 3 show narrow, vertical zones of low-resistivity, separated by broad horizontal areas of higher resistivity at depths of ∼3–7 km that support the convective model of heat transport described by *Bibby et al.* [1995]. The vertical low-resistivity zones appear to be images of the stable convection plumes. However, the observation that some of the plumes are offset from the surface geothermal fields indicate that geological structure in the upper crust also plays an important role in the heat transport and mass flow within the TVZ.

[18] Specifically, why is a vertical, low-resistivity plume located directly beneath Rotokawa, while at Ohaaki a low-resistivity connection to depth appears to be offset to the north-west? *Wood et al.* [2001] suggested that the difference in the basement permeability at Kawerau (Figure S7) and Ohaaki geothermal fields was a consequence of variations in greywacke lithology (geochemistry) between these two locations. Both Ohaaki and Kawerau are located ∼5 km from the eastern rift margin, and are the only geothermal fields in the TVZ with wells that penetrate greywacke basement at shallow depths (1–2.5 km). *Wood et al.* [2001] argue that brittle fractures are sustained at higher temperatures and depths in the andesite-rhyolite derived greywacke at Kawerau, compared to the more ductile granite-rhyolite derived greywacke at Ohaaki. At Rotokawa, located ∼8 km

from the eastern rift margin, greywacke is encountered in only two deep wells [*Rae*, 2007]. However, a cluster of earthquakes that locate in a resistive zone directly beneath the geothermal field at ~2–3 km depths (profile C in Figure 3) suggests that fracture permeability exists and is feeding high-temperature fluids into the system from below. The occurrence of seismicity within a resistive region beneath Rotokawa was also observed in an independent MT and passive-seismic survey [*Heise et al.*, 2008], and strongly supports the inference that deep (>3 km) fluid up-flow is located directly beneath the Rotokawa geothermal field.

[19] Alternatively, could the vertical low-resistivity plumes observed in the MT models be associated with shallow magmatic intrusions? For instance, a dioritic pluton was drilled at ~2.5 km depth at Ngatamariki, in the same area as the low-resistivity plume imaged beneath the geothermal field (profile G in Figure 3). However, localized intrusions at shallow depth can provide heat for only ~10^4 years [*Norton and Knight*, 1977], and the intrusion at Ngatamariki has a crystallization age of 550 ka [*Arehart et al.*, 2002]. Further, a lack of hydrothermal alteration in the overlying Whakamaru ignimbrite (330 ka) indicates that the Ngatamariki diorite had cooled prior to the emplacement of the ignimbrite, and does not comprise the heat source for the present geothermal system [*Arehart et al.*, 2002].

[20] *Bibby et al.* [1995] suggest that convection will distribute heat input from deep magmatic intrusions throughout the entire system, and consequently a one-to-one relationship between intrusive heat sources and geothermal fields is unlikely. Although it remains possible that in the ductile region of the crust (below ~6–7 km) zones of partial melt bulge upwards at the base of the low-resistivity plumes seen in these MT models (Figure 4). However, the most plausible interpretation of the vertical zones of low-resistivity between 3 and 7 km depth, where the pressure regime is expected to be near hydrostatic, is that they represent convection plumes of hot-fluid within fracture-permeability (shown schematically in Figure S8). These high temperature (>~330°C at Rotokawa) saline fluids will form an electrically conducting medium, which combined with hydrothermal alteration of the surrounding country rock, will lower the resistivity of the plume compared with adjacent regions of cold meteoric recharge. In the near-surface, variations in geological structure, horizontal permeability and groundwater flow may all play a role to direct these upwelling fluids to the locations of the geothermal fields.

5. Conclusions

[21] MT measurements in the south-eastern TVZ show compelling evidence that support a model of hydrothermal convection within the upper ~6–7 km. However, significant along-strike variation is seen in the resistivity models, indicating that heat flow and mass transport is 3-D. While questions remain, our MT array has for the first-time imaged the connections between the near-surface hydrothermal systems and the underlying magmatic systems that drive the TVZ's extraordinarily high heat flux.

[22] **Acknowledgments.** Cooperation from the majority of landowners in the survey area is greatly appreciated. We thank Weerachai Siripunvaraporn for use of his 3-D inversion program, WSINV3DMT. This research was funded by the New Zealand Ministry of Science and Innovation.

[23] The Editor wishes to thank Olivier Bachmann and two anonymous reviewers for their assistance in evaluating this paper.

References

Arehart, G. B., B. W. Christenson, C. P. Wood, K. A. Foland, and P. R. L. Browne (2002), Timing of volcanic, plutonic and geothermal activity at Ngatamariki, New Zealand, *J. Volcanol. Geotherm. Res.*, *116*, 201–214, doi:10.1016/S0377-0273(01)00315-8.

Bibby, H. M., T. G. Caldwell, F. J. Davey, and T. H. Webb (1995), Geophysical evidence on the structure of the Taupo Volcanic Zone and its hydrothermal circulation, *J. Volcanol. Geotherm. Res.*, *68*, 29–58, doi:10.1016/0377-0273(95)00007-H.

Bibby, H. M., G. F. Risk, T. G. Caldwell, and S. L. Bennie (2005), Misinterpretation of electrical resistivity data in geothermal prospecting: A case study from the Taupo Volcanic Zone, paper presented at World Geothermal Congress 2005, Int. Geotherm. Assoc., Antalya, Turkey.

Bignall, G. (2010), Hotter and deeper: New Zealand's research programme to harness its deep geothermal resources, paper presented at World Geothermal Congress 2010, Int. Geotherm. Assoc., Bali, Indonesia.

Bryan, C. J., S. Sherburn, H. M. Bibby, S. C. Bannister, and A. W. Hurst (1999), Shallow seismicity of the central Taupo Volcanic Zone, New Zealand: Its distribution and nature, *N.Z. J. Geol. Geophys.*, *42*, 533–542, doi:10.1080/00288306.1999.9514859.

Caldwell, T. G., H. M. Bibby, and C. Brown (2004), The magnetotelluric phase tensor, *Geophys. J. Int.*, *158*, 457–469, doi:10.1111/j.1365-246X.2004.02281.x.

Gamble, T. D., W. M. Goubeau, and J. Clarke (1979), Magnetotellurics with a remote reference, *Geophysics*, *44*, 53–68, doi:10.1190/1.1440923.

Harrison, A. J., and R. S. White (2006), Lithospheric structure of an active backarc basin: The Taupo Volcanic Zone, New Zealand, *Geophys. J. Int.*, *167*, 968–990, doi:10.1111/j.1365-246X.2006.03166.x.

Heise, W., H. M. Bibby, T. G. Caldwell, S. C. Bannister, Y. Ogawa, S. Takakura, and T. Uchida (2007), Melt distribution beneath a young continental rift: The Taupo volcanic zone, New Zealand, *Geophys. Res. Lett.*, *34*, L14313, doi:10.1029/2007GL029629.

Heise, W., T. G. Caldwell, H. M. Bibby, and S. C. Bannister (2008), Three-dimensional modelling of magnetotelluric data from the Rotokawa geothermal field, Taupo Volcanic Zone, New Zealand, *Geophys. J. Int.*, *173*, 740–750, doi:10.1111/j.1365-246X.2008.03737.x.

Heise, W., T. G. Caldwell, H. M. Bibby, and S. L. Bennie (2010), Three-dimensional electrical resistivity image of magma beneath an active continental rift, Taupo Volcanic Zone, New Zealand, *Geophys. Res. Lett.*, *37*, L10301, doi:10.1029/2010GL043110.

Hunt, T. M., and C. Harms (1990), Gravity survey of the Rotokawa geothermal field, in *Proceedings of the 12th New Zealand Geothermal Workshop*, edited by C. C. Harvey, pp. 91–96, Geotherm. Inst., Auckland, New Zealand.

Ingham, M. (2005), Deep electrical structure of the Central Volcanic Region and Taupo Volcanic Zone, New Zealand, *Earth Planets Space*, *57*, 591–603.

Kissling, W. M., and G. J. Weir (2005), The spatial distribution of the geothermal fields in the Taupo Volcanic Zone, New Zealand, *J. Volcanol. Geotherm. Res.*, *145*, 136–150, doi:10.1016/j.jvolgeores.2005.01.006.

Li, S., M. J. Unsworth, J. R. Booker, W. Wei, H. Tan, and A. G. Jones (2003), Partial melt of aqueous fluid in the mid-crust of southern Tibet? Constraints from INDEPTH magnetotelluric data, *Geophys. J. Int.*, *153*, 289–304, doi:10.1046/j.1365-246X.2003.01850.x.

McLellan, J. G., N. H. S. Oliver, B. E. Hobbs, and J. V. Rowland (2010), Modelling fluid convection stability in continental faulted rifts with applications to the Taupo Volcanic Zone, New Zealand, *J. Volcanol. Geotherm. Res.*, *190*, 109–122, doi:10.1016/j.jvolgeores.2009.11.015.

Nairn, I. A., P. R. Shane, J. W. Cole, G. L. Leonard, S. Self, and N. Pearson (2004), Rhyolite magma processes of the ~AD 1315 Kaharoa eruption episode, Tarawera volcano, New Zealand, *J. Volcanol. Geotherm. Res.*, *131*, 265–294, doi:10.1016/S0377-0273(03)00381-0.

Norton, D., and J. E. Knight (1977), Transport phenomena in hydrothermal systems: Cooling plutons, *Am. J. Sci.*, *277*, 937–981, doi:10.2475/ajs.277.8.937.

Ogawa, Y., H. M. Bibby, T. G. Caldwell, S. Takakura, T. Uchida, N. Matsushima, S. L. Bennie, T. Tosha, and Y. Nishi (1999), Wide-band magnetotelluric measurements across the Taupo Volcanic Zone, New Zealand: Preliminary results, *Geophys. Res. Lett.*, *26*, 3673–3676, doi:10.1029/1999GL010914.

Parkinson, W. D. (1962), The influence of continents and oceans on geomagnetic variations, *Geophys. J. R. Astron. Soc.*, *6*, 411–449.

Rae, A. (2007), Rotokawa geology and geophysics, *Consult. Rep. 2007/83*, 11 pp., GNS Sci., Lower Hutt, New Zealand.

Robinson, R., E. G. C. Smith, and J. H. Latter (1981), Seismic studies of the crust under the hydrothermal areas of the Taupo Volcanic Zone, New Zealand, *J. Volcanol. Geotherm. Res.*, *9*, 253–267, doi:10.1016/0377-0273(81)90007-X.

Rodi, W., and R. L. Mackie (2001), Nonlinear conjugate gradients algorithm for 2-D magnetotelluric inversion, *Geophysics*, *66*, 174–187, doi:10.1190/1.1444893.

Siripunvaraporn, W., G. Egbert, Y. Lenbury, and M. Uyeshima (2005), Three-dimensional Magnetotelluric inversion: Data-space method, *Phys. Earth Planet. Inter.*, *150*, 3–14, doi:10.1016/j.pepi.2004.08.023.

Stanley, W. D., W. D. Mooney, and G. S. Fuis (1990), Deep crustal structure of the Cascade range and surrounding regions from seismic refraction and magnetotelluric data, *J. Geophys. Res.*, *95*, 19,419–19,438, doi:10.1029/JB095iB12p19419.

Sutton, A. N., S. Blake, C. J. N. Wilson, and B. L. A. Charlier (2000), Late quaternary evolution of a hyperactive rhyolite magmatic system: Taupo volcanic centre, New Zealand, *J. Geol. Soc.*, *157*, 537–552, doi:10.1144/jgs.157.3.537.

Wilson, C. J. N., and G. S. Leonard (2008), Slumbering giants, in *A Continent on the Move: New Zealand Geoscience Into the 21st Century*, *Misc. Publ.*, vol. 124, edited by I. J. Graham, pp. 166–169, Geol. Soc. of N. Z., Wellington, New Zealand.

Wilson, C. J. N., B. F. Houghton, M. O. McWilliams, M. A. Lanphere, S. D. Weaver, and R. M. Briggs (1995), Volcanic and structural evolution of Taupo Volcanic Zone, New Zealand: A review, *J. Volcanol. Geotherm. Res.*, *68*, 1–28, doi:10.1016/0377-0273(95)00006-G.

Wood, C. P., R. L. Brathwaite, and M. D. Rosenberg (2001), Basement structure, lithology and permeability at Kawerau and Ohaaki geothermal fields, New Zealand, *Geothermics*, *30*, 461–481, doi:10.1016/S0375-6505(01)00003-7.

S. L. Bennie, E. A. Bertrand, T. G. Caldwell, and G. J. Hill, GNS Science, 1 Fairway Dr., Avalon, Lower Hutt 5010, New Zealand. (t.bertrand@gns.cri.nz)

N. Cozens, New Zealand Petroleum and Minerals, 33 Bowen St., Wellington, 6140, New Zealand.

S. A. Onacha, G. A. Ryan, C. Walter, P. Wameyo, and A. Zaino, IESE, University of Auckland, Private Bag 92019, Auckland 1142, New Zealand.

E. L. Wallin, Pacific Northwest National Laboratory, PO Box 999, Richland, Washington 99352, USA.